Improvement I-V characteristics of (GaAs/Ge) heterojunction at different thicknesses and annealing temperatures by thermal evaporation method

I. N. Kashkool[a], Saif Khalel Jasim[b,*] A. K. Mohammed[a], M. T. Abd[a], and A. M. Shano[a]

[a]*Department of Radiological Tech., Bilad Alrafidain University College, Diyala, 32001, Iraq.*
[b]*Ministry of Education. Diyala Education Directorate, Diyala, Iraq.*
[*]*e-mail: saifalaosy@gmail.com*

Received 14 March 2025; accepted 19 June 2026

In the present work we are reporting the preparation conditions of GaAs thin films and the technique employed to produce films deposited on Ge wafers substrate at constant substrate temperature by thermal evaporation method. Also it includes photovoltaic measurements which are presented by current voltage characteristics, photocurrent, shortcircuit, open - circuit voltage of GaAs/Ge heterojunction, at room temperature and different annealing temperatures. All the samples were prepared under constant conditions (pressure, substrate temperature and rate of deposition); the main parameters that control the nature of the film properties are thickness (0.4, 0.7, 1.0 and 1.5 μm) and annealing temperature (473 and 523 K). The dark current decreases with increasing of thickness; whereas increases slightly with increasing of annealing temperatures. Under illumination, the photocurrent increases with increasing of annealing temperatures and decreases with increasing of thickness except at thickness equal to 1.5 μm. There is a linear increasing in the first part of the relation between Isc and Voc with incident power intensity and then the saturation region appeared. The Isc and Voc decrease with increasing of thickness, while increase with increase of annealing temperatures.

Keywords: GaAs; solar cell; I_V characteristics; thickness; thin films.

DOI: https://doi.org/10.31349/RevMexFis.72.061007

1. Introduction

Germanium (Ge) has been one of the most studied materials as its properties benefit many applications. Ge was the choice of material used in the first bipolar invented transistor in 1949 by Bardeen, Brattain, and Shockley [1,2]. Due to its small energy band gap 0.66 eV, Ge is also used in optical and optoelectronic devices, (such as photodetectors, solar cells,and waveguides) [3]. In addition, Ge films can be grown epitaxially on the GaAs heterostructures typically used for fabrication of a number of types of electronic devices, such as photodetectors, diodes and sensors of temperature, magnetic field and strain [4,5]. Ge and GaAs have almost the same lattice parameter at room temperature [6]. GaAs/Ge epitaxial heterostructures have received a great deal of attention as starting materials for the fabrication of space quality solar cells and their potential application in electronic and optoelectronic devices.

Due to its high mechanical strength, Ge is an optimized substrate material in terms of its power - to power ratio for high efficiency GaAs/Ge photovoltaic devices. As large area, minority carrier devices, III-V/Ge cells are extremely sensitive to defects [7,8]. GaAs devices fabricated on a Ge substrate can have higher resistance to thermal burn out than those fabricated on a GaAs substrate, as Ge has thermal conductivity compared to GaAs [9,10]. The devices on Ge will be more economical as the cost of Ge wafers is less than that of GaAs wafers [11,12]. The elimination of antiphase domains (APDs), which are characteristic of polar-on-non polar epitaxy, and suppression of large - scale inter diffusion across the GaAs/Ge heterointerface remain key challenges for increase yield, reliability, and performance [13,14].

From a commercial perspective, the utilization of thermal evaporation for GaAs/Ge heterojunction fabrication offers a highly cost-effective and scalable alternative to expensive epitaxy techniques like MBE or MOCVD, making it attractive for mass-produced terrestrial and space solar applications [15]. In the present work we are reporting the preparation conditions of GaAs thin films and the technique employed to produce films deposited on Ge wafers substrate at constant substrate temperature by thermal evaporation method [16]. Also, it includes photovoltaic measurements which are presented by current - voltage characteristics, photocurrent, short - circuit, open - circuit voltage of GaAs/Ge heterojunction, at room temperature and different annealing temperatures.

2. Experimental procedure

Two types of substrates were used in this study: glass slides which were used to study the structural, electrical and optical properties of GaAs films; and p-type Ge wafer substrate with crystal orientation (100), with electrical resistivity of 55.5 Ω·cm, free carriers concentration 3.3×10^{13} cm^{-3} and thickness of 450 μm. The Ge substrate forms with GaAs film the heterojunction. To ensure accurate electrical characteri-

zation of the GaAs layer and avoid parasitic conduction from the substrate, separate GaAs films were deposited on insulating glass slides under identical conditions for Hall effect measurements. Flash evaporation technique was used to prepare GaAs films to avoid the segregation problem. This technique, which involves instantaneous evaporation of the material with minimum time of contact with the evaporator, has been successfully used for growing precisely stoichiometric films of compounds whose constituents have widely different vapor pressures.

In this technique, the finely powdered evaporating material is allowed to drop grain by grain onto a hot surface whose temperature is maintained well above the evaporation temperature of the least volatile constituent of the evaporant. The preparation of GaAs films with satisfactorily reproducible properties demands special technological procedures. Therefore, flash evaporation techniques were chosen in the present investigation [17,18]. The required weight of GaAs powder was charged into a funnel structure which was fixed in the holder and the boat was mounted under the funnel between two electrodes in the vacuum chamber. The substrates were fixed on a spherical holder and placed in position at height of about 12 cm above the boat.

Before starting the evaporation process, the substrate was heated to about 433 K. The temperature was monitored by using a digital thermometer. When the system was pumped down to a vacuum of 10^{-5} mbar, an electric current was passed through the boat gradually to prevent breaking the boat, when the boat temperature reached the required temperature the deposition process starts with constant deposition rate. After these steps the current supply was switched off and the samples were left in the high vacuum for one day, and then the air was admitted to the chamber, and the films were taken out from the coating unit and kept in the vacuum desiccators until the measurements were made.

All the samples were prepared under constant conditions (pressure, substrate temperature and rate of deposition); the main parameters that control the nature of the film properties are thickness (0.4, 0.7, 1.0 and 1.5 μm) and annealing temperature (473 and 523 K). There are many methods used to determine the film thickness. In this part two experimental methods of thickness measurements were used. Weighting Method I-V measurements have been done under illumination for the GaAs/Ge heterojunction which was prepared with different thicknesses and annealing temperatures at forward and reverse conditions with different intensities (30-105 mW/cm^2) by using Halogen lamp type Philips of 120 W. The current-voltage measurements in the dark were done for the GaAs/Ge heterojunction by using Keithley digital electrometer 616 and D.C. power supply. The bias voltage was varied in the range of (0-1 V) in the case of forward and reverse bias.

3. Results and discussions

3.1. Structural properties

The structural properties of the deposited GaAs thin films were investigated using X-ray diffraction (XRD). As shown in Fig. 1, the XRD patterns exhibit three distinct peaks at 2θ values of approximately 27.5°, 45.5°, and 53.5°, corresponding to the (111), (220), and (311) planes of the cubic zincblende structure.

The structural properties of the deposited GaAs thin films were investigated using X-ray diffraction (XRD). As shown in Fig. 1, the XRD patterns exhibit three distinct peaks at 2θ values of approximately 27.5°, 45.5°, and 53.5°, corresponding to the (111), (220), and (311) planes of the cubic zincblende structure.

A significant increase in peak intensity and a reduction in the Full Width at Half Maximum (FWHM) were observed as the annealing temperature increased from 303 K to 523 K. This indicates an enhancement in crystallinity and an increase in grain size, as detailed in Table I. The improved grain size

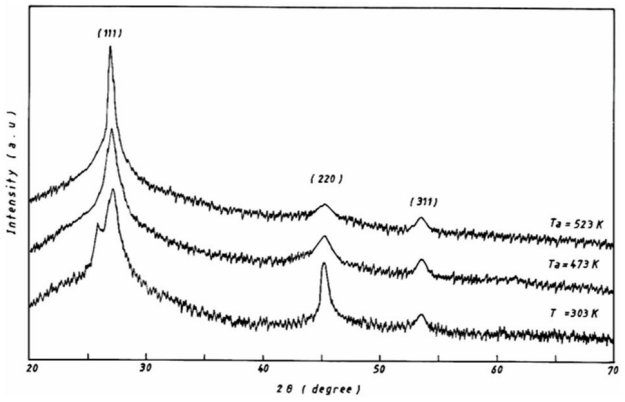


FIGURE 1. X-ray diffraction patterns of GaAs thin films (1.0 μm thickness) deposited on Ge substrates at room temperature (303 K) and after annealing at different temperatures (473 K and 523 K).

TABLE I. Structural parameters of GaAs thin films at different annealing temperatures.

D(Å)	(hkl)	a(Å)	d_{exp} (Å)	2θ (degree)
GaAs Films at T = 303 K				
37.550	111	5.611	3.240	27.5
107.352	220	5.632	1.991	45.5
97.007	311	5.674	1.711	53.5
GaAs Films at T_a = 473 K				
54.881	111	5.611	3.240	27.5
48.481	220	5.632	1.991	45.5
103.474	311	5.674	1.711	53.5
GaAs Films at T_a = 523 K				
155.211	111	5.611	3.240	27.5
65.345	220	5.632	1.991	45.5
118.908	311	5.674	1.711	53.5

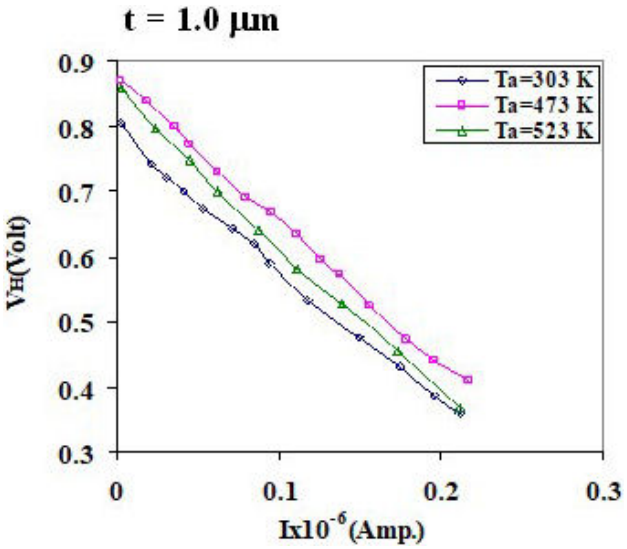


FIGURE 2. Hall potential (V_H) as a function of current for thin GaAs films of thickness (1.0 μm) at room temperature and different annealing temperatures (473 K and 523 K).

(reaching 155.2 Å at 523 K) reduces grain boundary scattering and recombination centers, which directly correlates with the enhanced I-V characteristics of the GaAs/Ge heterojunction.

3.2. Hall effect measurements

Hall effect measurements on GaAs films deposited on glass substrates confirmed n-type conductivity with a negative Hall coefficient. Figure 2 displays the linear Hall voltage (V_H) and current for the 1.0 μm film, where the increase in V_H with annealing temperature (T_a) indicates a modification in free carrier density and mobility. These results provide experimental evidence for the formation of an n-GaAs/p-Ge heterojunction when deposited on p-Ge wafers.

3.3. Characteristics for GaAs/Ge Heterojunction under dark

One of the important parameters of diode measurement is a current-voltage characteristic which explains the behavior of the resultant current with the applied forward and reverse bias voltages. Figure 3 shows I-V characteristics for GaAs/Ge heterojunction at forward and reverse bias voltages for different thicknesses and annealing temperatures.

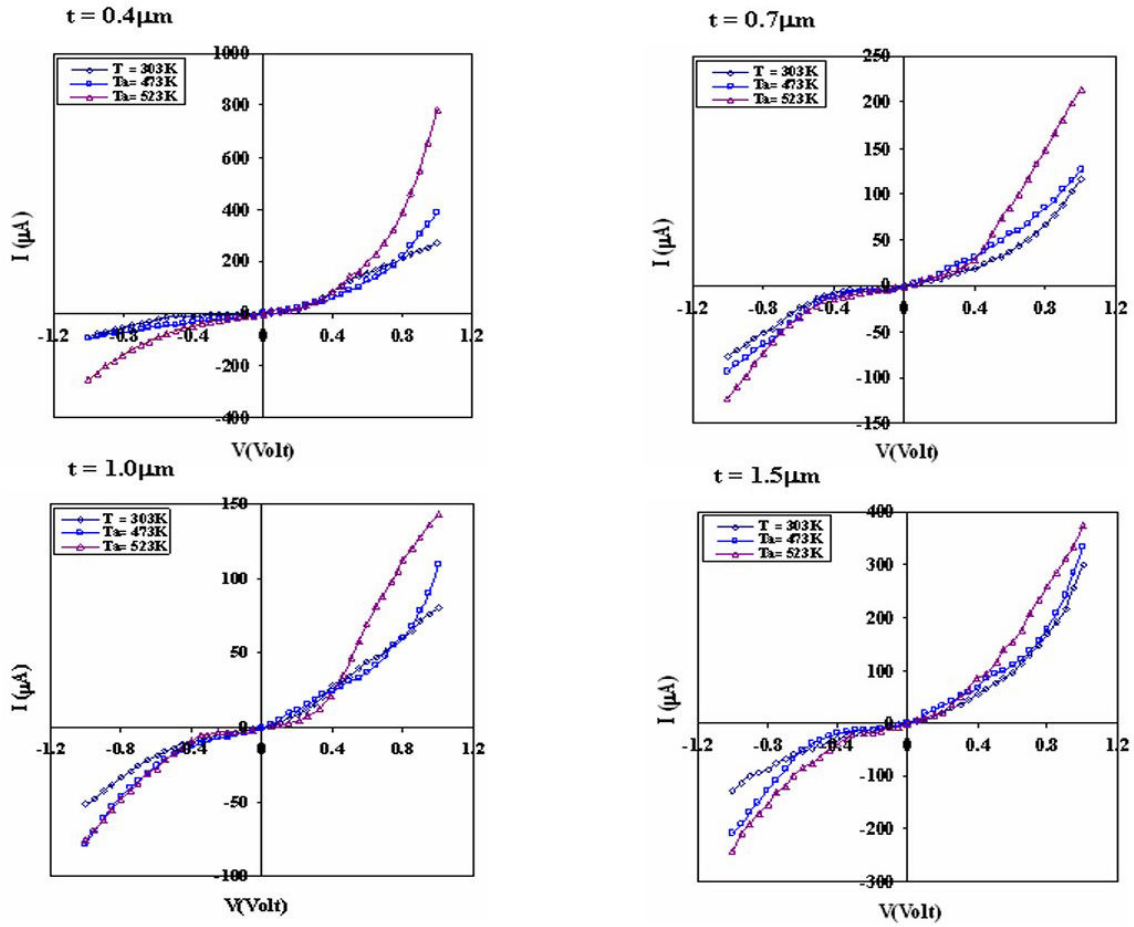


FIGURE 3. I-V characteristics for GaAs/Ge heterojunction at forward and reverse bias voltages for different thicknesses and annealing temperatures.

In general, the forward dark current is generated due to the flow of majority carriers and the applied voltage injects majority carriers which lead to the decrease of the built - in potential, as well as the width of the depletion layer. As the majority and minority carrier concentration is higher than the intrinsic carrier concentration ($n_i^2 < np$) which generate the recombination current at the low voltage region (0-0.3 V). This is because the excitation of electrons from valence band (V.B.) to conduction band (C.B.) will recombine them with the holes which are found at the V.B., and this is observed by the little increase in recombination current at low voltage region [15,16]. On the other hand, tunnelling current is present at the high voltage region (> 0.3 V). After that there is a fast exponential increase in the current magnitude with increasing of the voltage and this is called diffusion current, which dominates [19].

The reverse bias current also contains two regions. In the first region of low voltages (< 0.3 V), the current slightly increases with increasing of the applied voltage, and the generation current dominates, while at second high voltage region (> 0.3 V), the diffusion current dominates [20]. Also we can observe from this figure that the value of the current decreases with increasing of thickness of GaAs films which is attributed to evolving defects and dislocations that have an effect on the mobility of charge carriers. Also these defects evolutions allow energy levels to be within the energy gap, these defects are within the depletion region and act as active recombination centers, and consequently they decrease current flow across the junction. This behavior is similar for all the film thicknesses except at thickness equal to 1.5 μm. We also observed that the current increases slightly with increasing of annealing temperature because the increasing of temperatures causes a rearrangement of the interface atoms and reduce the dangling bond which leads to improvement of the junction characteristics [21,22].

3.4. Short circuit current and open circuit voltage measurement for GaAs/Ge heterojunction

The variation of I_{sc} as a function of incident power intensity for GaAs/Ge heterojunction at different thicknesses (0.4, 0.7,

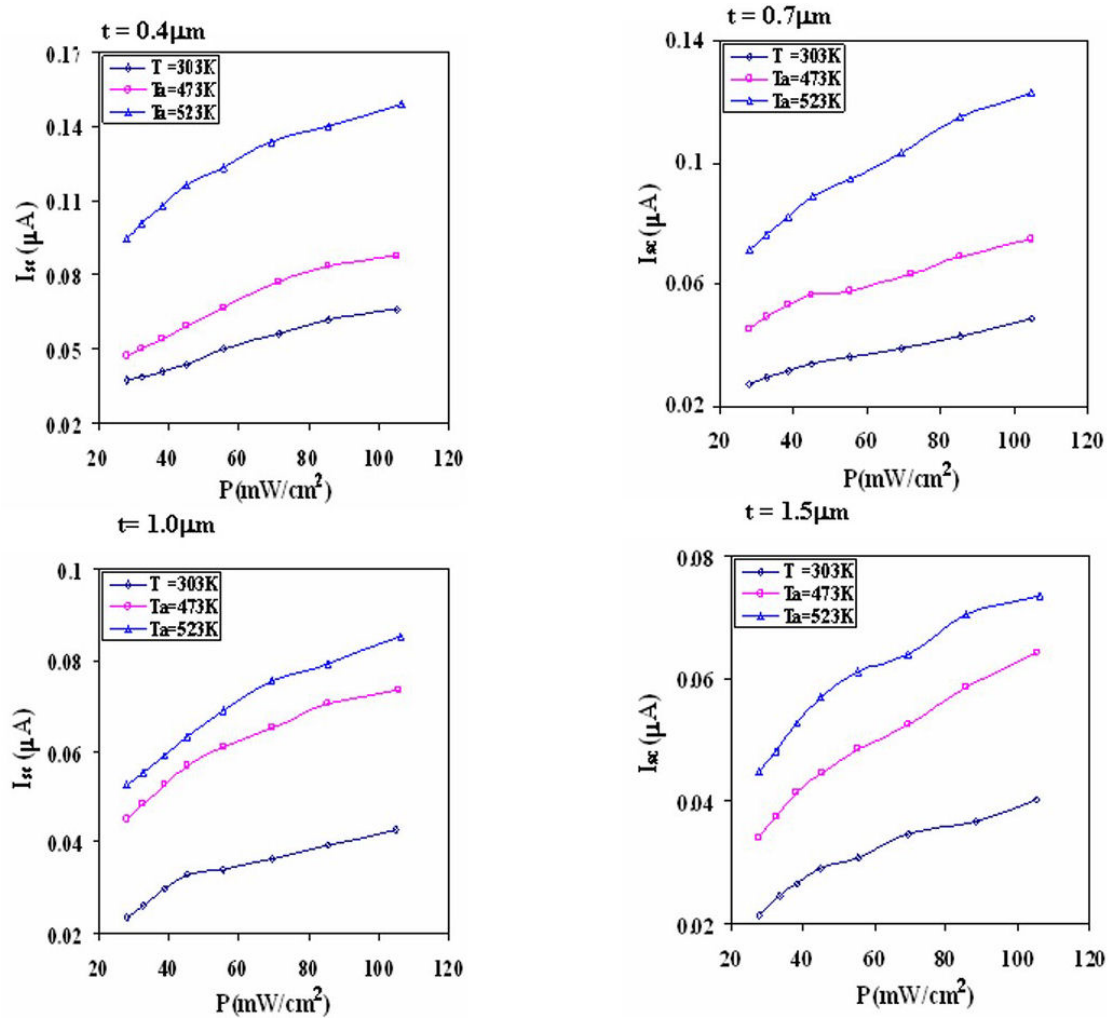


FIGURE 4. The variation of I_{sc} as a function of incident power intensity for GaAs/Ge heterojunction at different thicknesses and annealing temperatures.

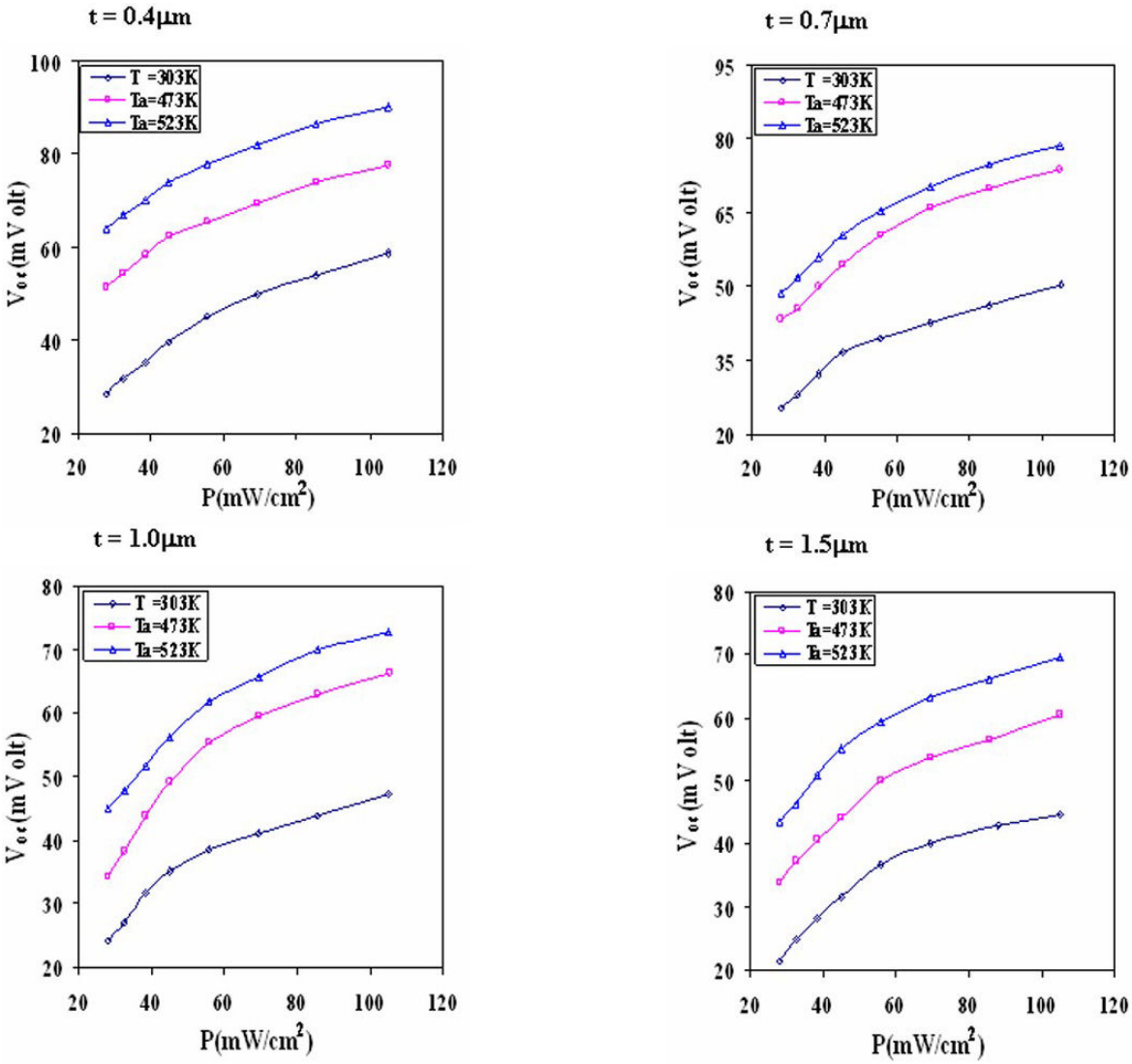


FIGURE 5. The variation of V_{oc} as a function of incident power intensity for GaAs/Ge heterojunction at different thicknesses and annealing temperatures.

1.0 and 1.5 μm) at R.T and annealing temperatures (473 and 523 K) is shown in Fig. 4.

We can observe from this figure that the I_{sc} increases with increasing of the incident power intensity. The behavior of I_{sc} is linear at the first portion and this is attributed to the incident power intensity. In the second portion there is a tendency to saturation with increasing of the incident power intensity at a limited range, due to the recombination effect [23,24]. We can observe that I_{sc} decreases with increasing of thickness of GaAs films about two times. This is attributed to the defects which act as capture centers to the generation of carriers, leading to an increase of the recombination process and a decrease of the current value. I_{sc} increases with increasing of annealing temperature due to the decrease of the defects by annealing and the improvement of the structure [25,26]. The observed enhancement in solar cell parameters via simple thermal evaporation underscores the potential for low-cost commercial photovoltaic devices.

The variation of V_{oc} as a function of power light intensity for GaAs/Ge heterojunction at different thicknesses (0.4, 0.7, 1.0 and 1.5 μm) and at R.T and annealing temperatures (473 and 523 K) is shown in Fig. 5.

Also we can divide this figure into two regions: a linear region at low illumination intensities, and a tendency for a saturation region at high illumination intensities. The V_{oc} decreases with increasing of thickness due to recombination processes at traps centers inside the materials or at the surface. The V_{oc} increases with increasing of annealing temperature due to the reduction of the defects and localized states and increasing of the mobility.

4. Conclusions

From the obtained results of the present work, we conclude that the mechanism of the forward current coincides with the recombination- tunneling mechanism. The dark current

decreases with increasing of thickness; whereas increases slightly with increasing of annealing temperatures.

Under illumination, the photocurrent increases with increasing of annealing temperatures and decreases with increasing of thickness except at thickness equal to 1.5 μm. There is a linear increasing in the first part of the relation between I_{sc} and V_{oc} with incident power intensity and then the saturation region appeared. The I_{sc} and V_{oc} decrease with increasing of thickness, while increase with increase of annealing temperatures. The results demonstrate that thermal evaporation is a viable, economical method for fabricating GaAs/Ge solar cells with promising performance, offering a significant reduction in production costs for large-scale energy applications.

Acknowledgment

The authors would like to thank the University of Diyala/College of Science/Department of Physics for the technical support to complete this work in their laboratories, and Universiti Sains Malaysia.

Conflict of interest

The authors declare that they have no conflict of interest.

1. Y. H. Hu, M. J. Li, Y. P. Zhou, H. Xi, and T. C. Hung, Multi-physics investigation of a GaAs solar cell based PV-TE hybrid system with a nanostructured front surface, *Sol. Energy* **224** (2021) 102-111. https://doi.org/10.1016/j.solener.2021.06.003
2. T. Y. Sabri, S. K. Jasim, A. A. Habeeb, and A. S. Jasim, Preparation and study Ag nanoparticles via PLAL technique: Influence of different number of pulses, *Int. J. Nanoelectron. Mater*. **17** (2024) 45-51. https://doi.org/10.58915/ijneam.v17i1.458
3. C. Wang, Z. Zhang, X. Jing, Z. Yang, and W. Xu, Optimization of multistage femtosecond laser drilling process using machine learning coupled with molecular dynamics, *Opt. Laser Technol*. **156** (2022) 108442. https://doi.org/10.1016/j.optlastec.2022.108442
4. E. S. Goh, T. P. Chen, C. Q. Sun, and Y. C. Liu, Thickness effect on the band gap and optical properties of germanium thin films, *J. Appl. Phys.* **107** (2010) 023506. https://doi.org/10.1063/1.3291103
5. C. Han *et al*., Microstructure evolution and ductility improvement of additively manufactured biodegradable zinc-magnesium alloys via annealing, *Int. J. Bioprint.* **10** (2024) 3034. https://doi.org/10.36922/ijb.3034
6. J. Peng *et al*., Numerical simulation and process parameter optimization of laser spot welding for ultra-thin sheets, *Opt. Laser Technol*. **193** (2026) 114240. https://doi.org/10.1016/j.optlastec.2025.114240
7. S. K. Jasim, A. M. Shano, and S. K. Adnan, Zinc oxide poly crystals heterojunction and infrared-blind UV-photodetector, *J. Nano-Electron. Phys.* **16** (2024) 01012. https://doi.org/10.21272/jnep.16(1).01012
8. Y. Zhang, Z. Zhang, X. Zhang, K. Wu, R. Riedel, D. Hu, and J. Sun, Machine learning guided design and ablation behavior of ZrC-TaC-SiC ternary coatings, *Corros. Sci*. **260** (2026) 113499. https://doi.org/10.1016/j.corsci.2025.113499
9. S. K. Jasim, S. M. A. Al Hussan, and M. T. Abd, Improving the mechanical properties of dental fillings by adding TiO_2 NPs prepared laser ablation, *BioNanoScience* **15** (2025) 330. https://doi.org/10.1007/s12668-025-01970-y
10. R. Kumar *et al*., Realization of high-quality InGaAs/GaAs quantum dot growth on Ge substrate and improvement of optical property through ex-situ ion implantation, *J. Lumin.* **223** (2020) 117208. https://doi.org/10.1016/j.jlumin.2020.117208
11. Y. Jiang, H. Shen, T. Pu, C. Zheng, Q. Tang, K. Gao, and Y. Liu, High efficiency multi-crystalline silicon solar cell with inverted pyramid nanostructure, *Sol. Energy* **142** (2017) 91-96. https://doi.org/10.1016/j.solener.2016.12.007
12. I. Hilmi, M. K. Adam, J. Purwadi, Q. M. B. Soesanto, and D. Y. Kusuma, Influence of annealing on the physical and optical properties of Ge thin films deposited using thermal evaporation, *J. Phys. Appl.* **7** (2025) 28-32. https://doi.org/10.14710/jpa.v7i2.24517
13. A. H. Ahmed, A. S. Jasima, and S. K. Jasim, Synthesis of gold nanoparticles by pulsed laser ablation and its study physical and mechanical properties, *Int. J. Nanoelectron. Mater*. **17** (2024) 634-644. https://doi.org/10.58915/ijneam.v17i4.1465
14. I. Demir, A. E. Kasapoğlu, H. F. Budak, E. Gür, and S. Elagoz, Influences of thickness and temperature of low temperature GaAs buffer layer on two-step MOVPE grown GaAs/Ge heterostructures, *Eur. Phys. J. Appl. Phys*. **90** (2020) 20301. https://doi.org/10.1051/epjap/2020190216
15. W. Kou, J. Gou, J. Gao, J. Zhu, Z. Li, and J. Wang, Effects of arc oscillation on interface behavior and properties of additive-manufactured 2319/5356 dissimilar aluminum alloy, *Mater. Today Commun*. **47** (2025) 113068. https://doi.org/10.1016/j.mtcomm.2025.113068
16. S. K. Jasim, S. M. A. A. Hussan, A. S. Noori, and A. A. Habeb, Determine surface plasmon resonance and effect parameters laser ablation on Cu and Zn nanoparticles, *AIP Conf. Proc*. **3219** (2024) 060008. https://doi.org/10.1063/5.0236469
17. Y. Zhou, W. Liu, S. Zhang, H. Liu, Z. Wu, and X. Wang, Eco-friendly flame-retardant phase-change composite films based on polyphosphazene/phosphorene hybrid foam and paraffin

wax for light/heat-dual-actuated shape memory, ACS *Appl. Mater. Interfaces* **16** (2024) 7754-7767. https://doi.org/10.1021/acsami.3c16953

18. J. Zhou *et al*., GaAs/GeSn/Ge n-i-p diodes and light emitting diodes formed via grafting, *J. Vac. Sci. Technol. B* **42** (2024). https://doi.org/10.1116/6.0003619

19. E. Erofeev and V. Kagadei, Formation of Ge/Cu ohmic contacts to n-GaAs with atomic hydrogen pre-annealing step, *Proc. SPIE* **7521** (2010) 176-181. https://doi.org/10.1117/12.853639

20. I. Kabacelik, M. Kulakci, and R. Turan, Structural and electrical analysis of poly-Ge films fabricated by e-beam evaporation for optoelectronic applications, *Mater. Sci. Semicond. Process.* **56** (2016) 368-372. https://doi.org/10.1016/j.mssp.2016.09.023

21. N. A. Pakhanov and M. Z. Shvarts, Designing of lightweight and ultrathin III-V/Ge solar cells for flexible space and terrestrial photovoltaic blankets, *Phys. Status Solidi A* **221** (2024) 2300709. https://doi.org/10.1002/pssa.202300709

22. R. Naik, A. Aparimita, D. Alagarasan, S. Varadharajaperumal, and R. Ganesan, Linear and nonlinear optical properties change in Ag/GeS heterostructure thin films by thermal annealing and laser irradiation, *Opt. Quantum Electron*. **52** (2020) 136. https://doi.org/10.1007/s11082-020-2245-6

23. X. Zhang, J. Sun, Y. Zhang et al., Machine learning for phase prediction of high entropy carbide ceramics from imbalanced data, *npj Comput. Mater*. (2026). https://doi.org/10.1038/s41524-025-01873-2

24. G. Cai, Y. Huang, Y. Qing, and R. D. K. Misra, Investigation of microstructure and texture evolution of nickel-saving duplex stainless steels containing Y, *J. Mater. Res. Technol*. (2026). https://doi.org/10.1016/j.jmrt.2026.01.109

25. Z. Zhang *et al*., Synergistic radiation effect of 300 MeV proton and heavy ion on electrical characteristics of β-Ga_2O_3 SBD, *IEEE Trans. Nucl. Sci*. (2026). https://doi.org/10.1109/TNS.2026.3666502

26. Y. Liu *et al*., Effect of annealing temperature on microstructure and properties of stainless steel/copper composite strips, *Adv. Compos. Hybrid Mater.* **9** (2026) 103. https://doi.org/10.1007/s42114-026-01648-3